Supplementary material for

One-shot battery degradation trajectory prediction with deep learning

Weihan Li[1,2*], Neil Sengupta[1], Philipp Dechent[1,2], David Howey[4,5], Anuradha Annaswamy[6], Dirk Uwe Sauer[1,2,3*]

[1]Chair for Electrochemical Energy Conversion and Storage Systems, Institute for Power Electronics and Electrical Drives (ISEA), RWTH Aachen University, Jägerstraße 17-19, 52066 Aachen, Germany
[2]Jülich Aachen Research Alliance, JARA-Energy, Templergraben 55, 52056 Aachen, Germany
[3]Helmholtz Institute Münster (HI MS), IEK-12, Forschungszentrum Jülich, 52425 Jülich, Germany
[4]Department of Engineering Science, University of Oxford, Parks Road, Oxford OX1 3PJ, UK
[5]The Faraday Institution, Harwell Campus, Didcot OX11 0RA, UK
[6]Department of Mechanical Engineering, Massachusetts Institute of Technology, 33 Massachusetts Ave, MA 02139 Cambridge, USA
*Correspondence: weihan.li@isea.rwth-aachen.de (W.L.), batteries@isea.rwth-aachen.de (D.U.S.)

Supplemental Items:

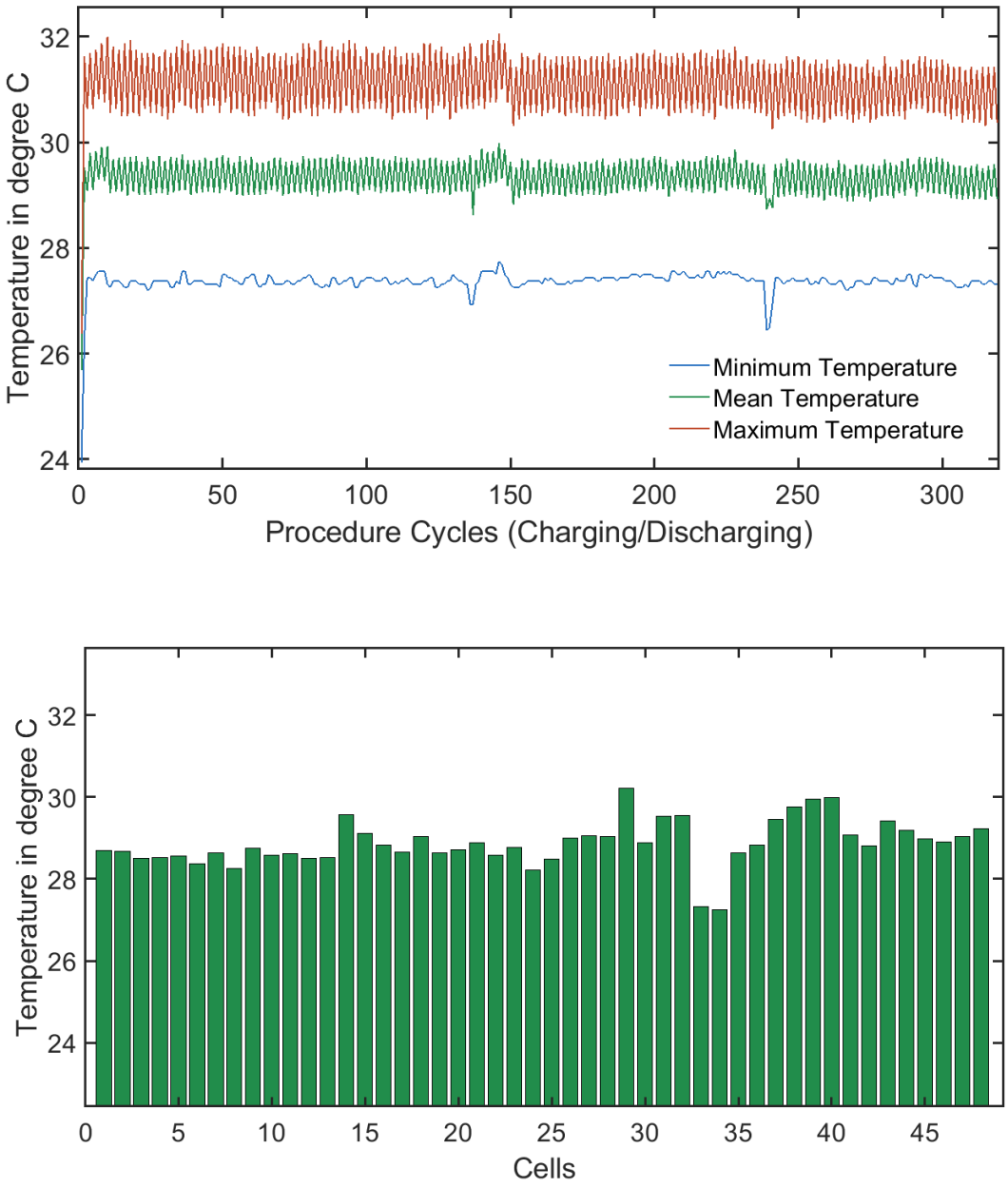

Figure S1. Analysis of the cell temperatures during the experiments. The First figure shows the minimum, mean and the maximum temperature of one cell (Test Cell 1) during one cycling round consisting of 158 charging and discharging processes. The second figure shows the average temperature that a cell experienced over its entire ageing process, for all 48 cells in the dataset.

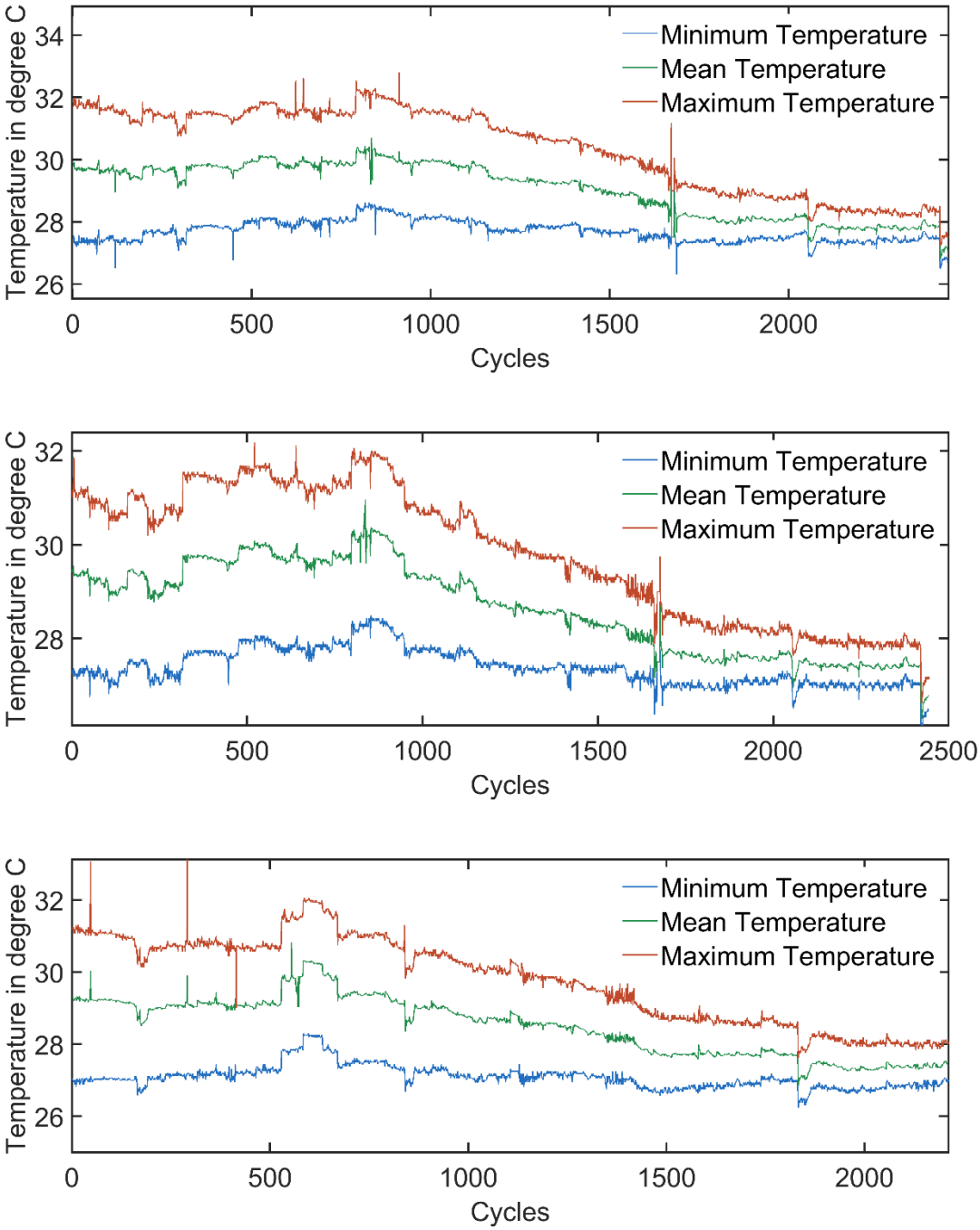

Figure S2. Analysis of the cell temperatures during the experiments. The minimum, mean and the maximum temperature development over the entire lifetime of 3 of the 5 test cells are shown in this figure. Possible sensor measurement errors have not been filtered for data completeness.

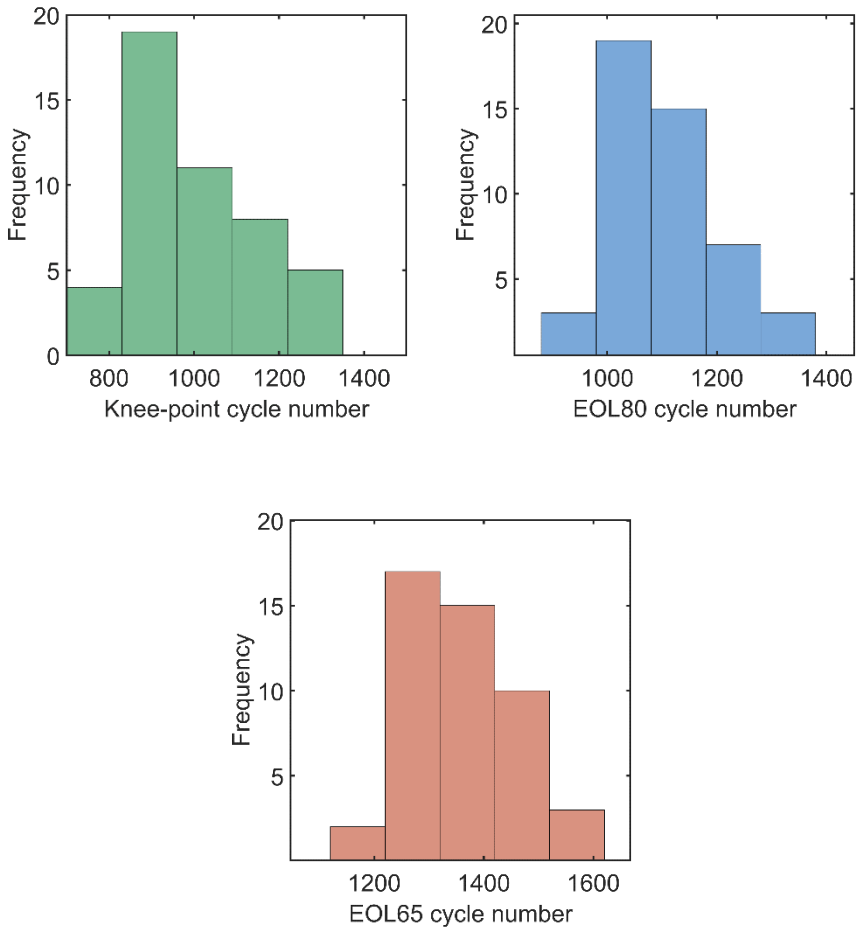

Figure S3. Histogram figures showing the variation in the cycle numbers of the 3 points of the interest of the cell across the dataset, namely the cycle numbers at which the different cells reach their knee-point, EOL80 criteria and EOL65 criteria.

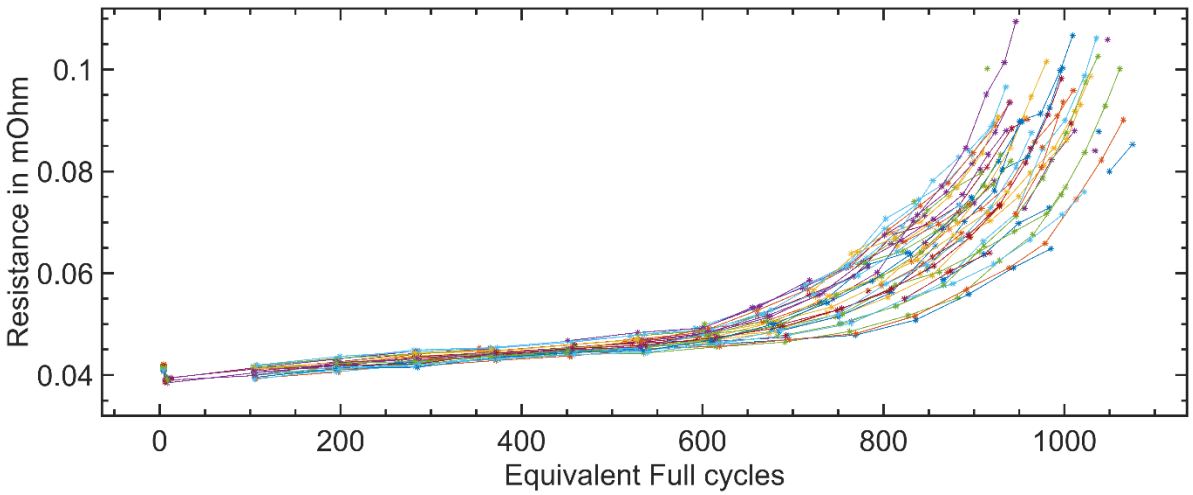

Figure S4. Progression of the pulse resistances of all the cells in the dataset, over their lifetime. The experiment was set up to measure 2 s pulse resistance for a 2 A discharge at 90% SOC. The x-axis is in equivalent full cycles, expanded to be for 100% depth of discharge. The internal resistance of the cell affects its ability to deliver power and a 100% increase in the resistance of the cell usually signifies the end of the first life.

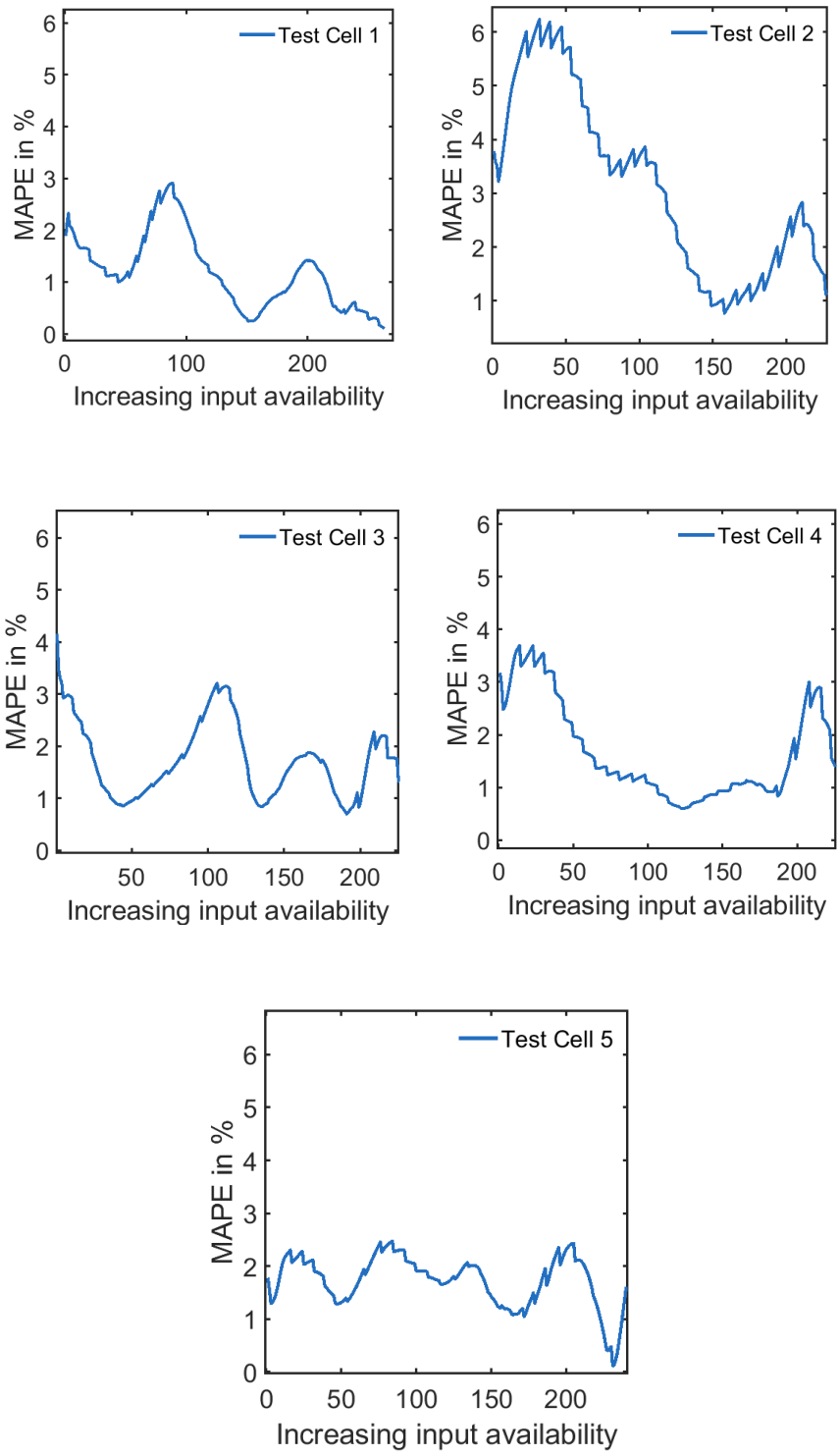

Figure S5. The progression of the MAPE over the lifetime of all five cells. The capacity history, in a number of samples, available to the model for prediction increases from left to right.

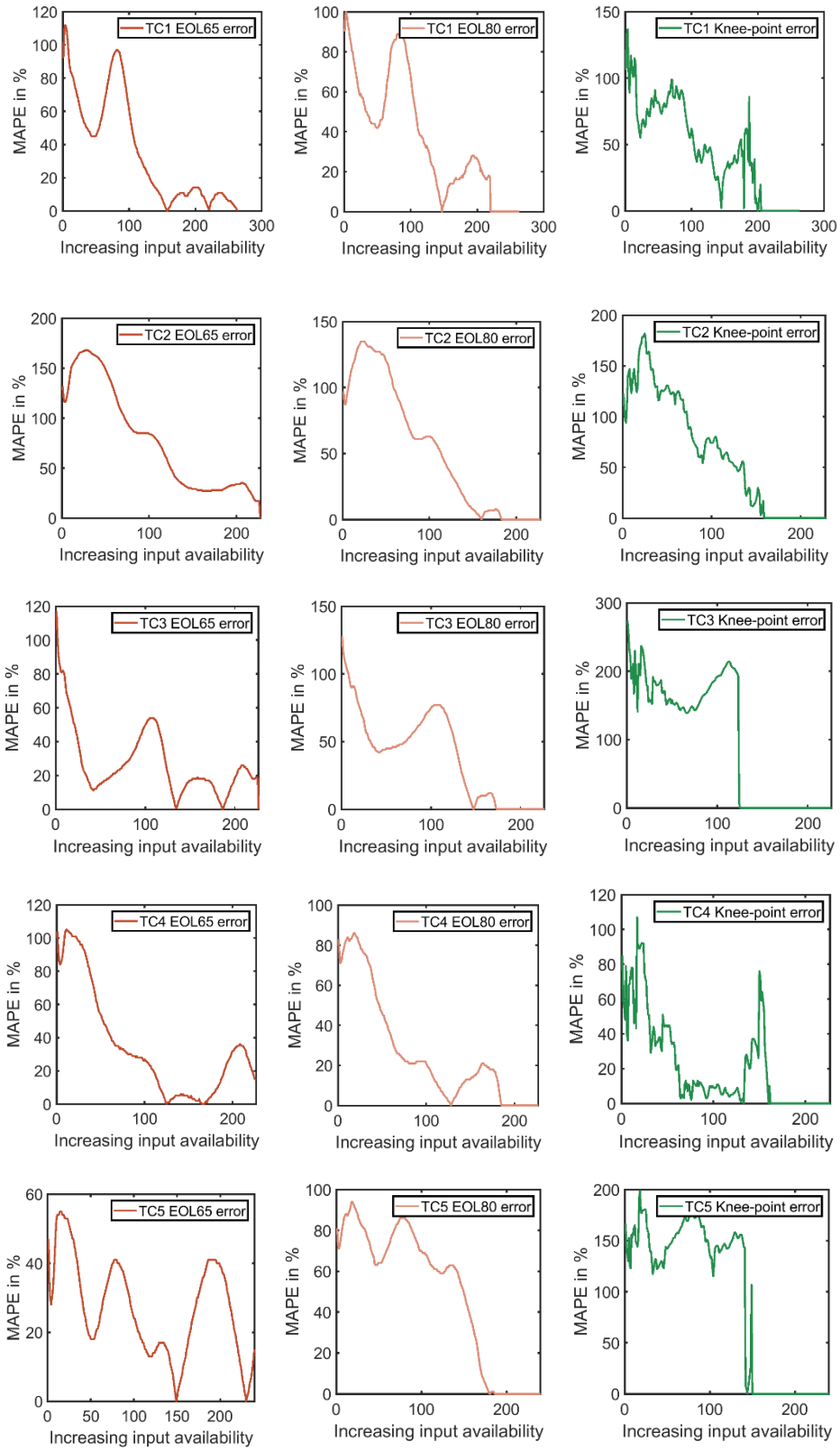

Figure S6. The EOL65, EOL80 and knee-point error progression chart of the five testing cells (TCs), over their lifetime. The input size, in a number of samples, increases from left to right.

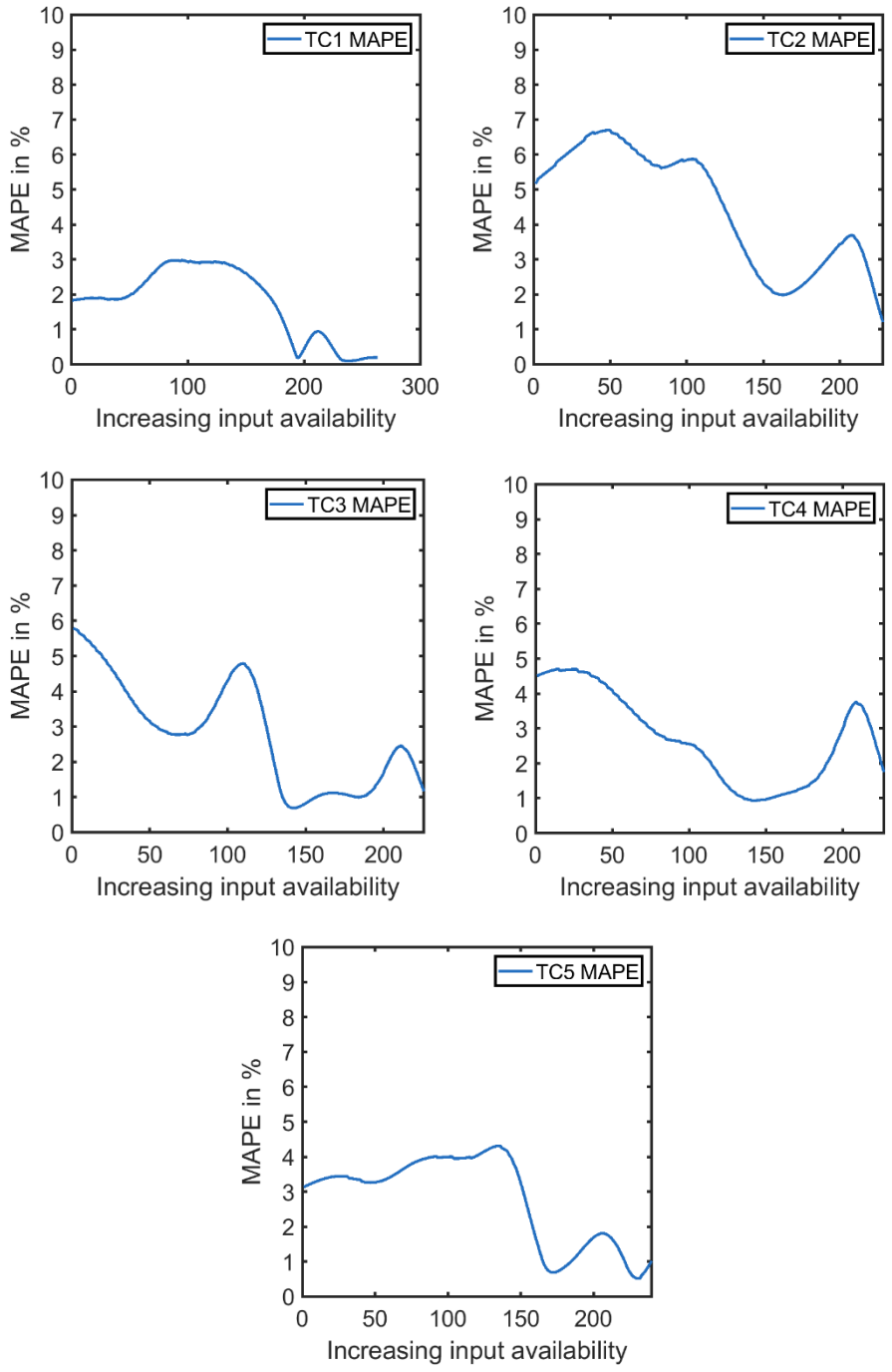

Figure S7. The progression of the MAPE over the lifetime of all five cells, as predicted with the iterative Benchmark LSTM model. The capacity history, in a number of samples, available to the model for prediction increases from left to right.

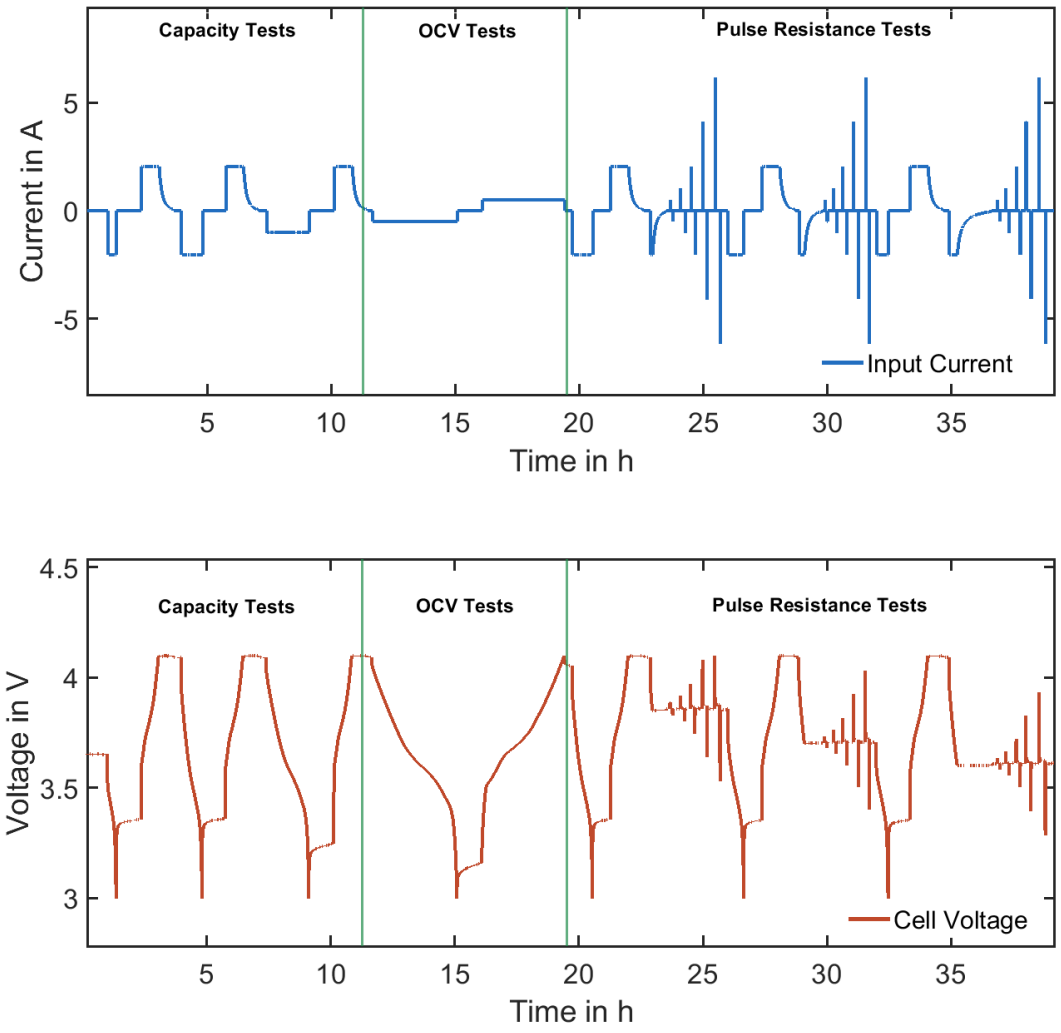

Figure S8. The current and voltage profiles respectively over the full characterization tests. The main three parts of the test, as highlighted, are the capacity measurements at two different C-rates, followed by a quasi-open-circuit-voltage (qOCV) measurement test and finally multi-pulse resistance tests at different SOCs.

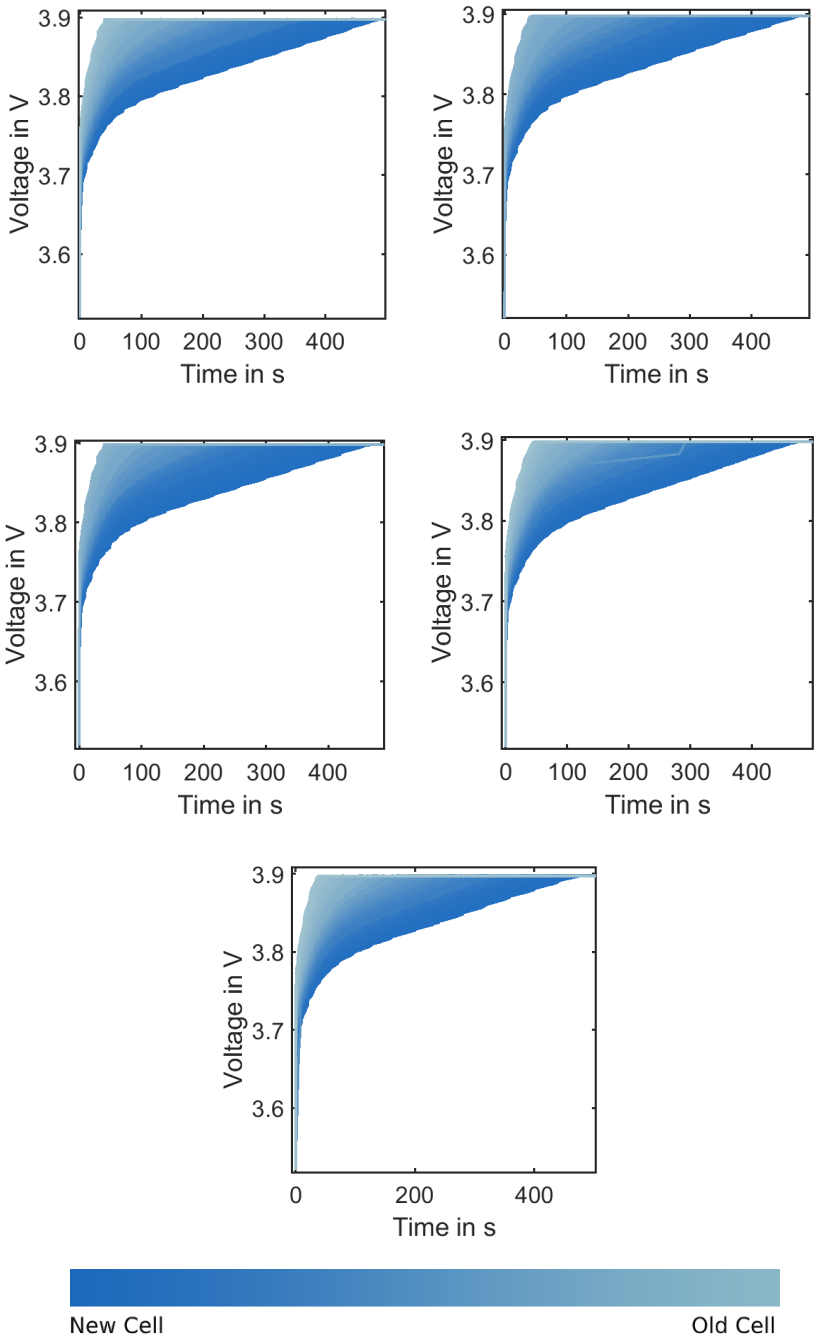

Figure S9. Voltage over time curves highlighting the changes during the constant current (CC) phase as cell ageing occurs, plotted for the five test cells. As cell capacity degrades, the maximum voltage for the end of the CC phase is reached much more quickly, for all of the cells.

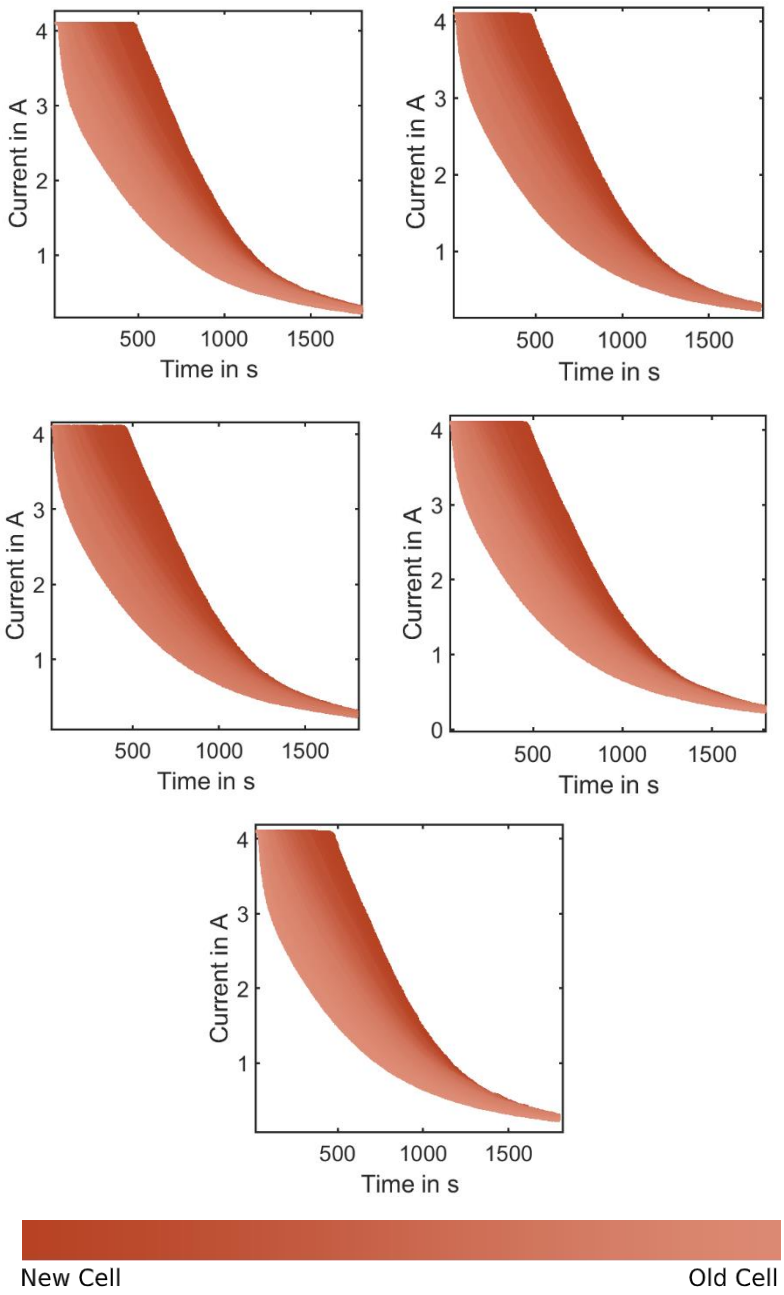

Figure S10. Current over time curves highlighting the changes during the constant voltage (CV) phase as cell ageing occurs, plotted for the five test cells. As cell capacity degrades, the CV phase starts earlier and lasts much longer, for all of the cells.

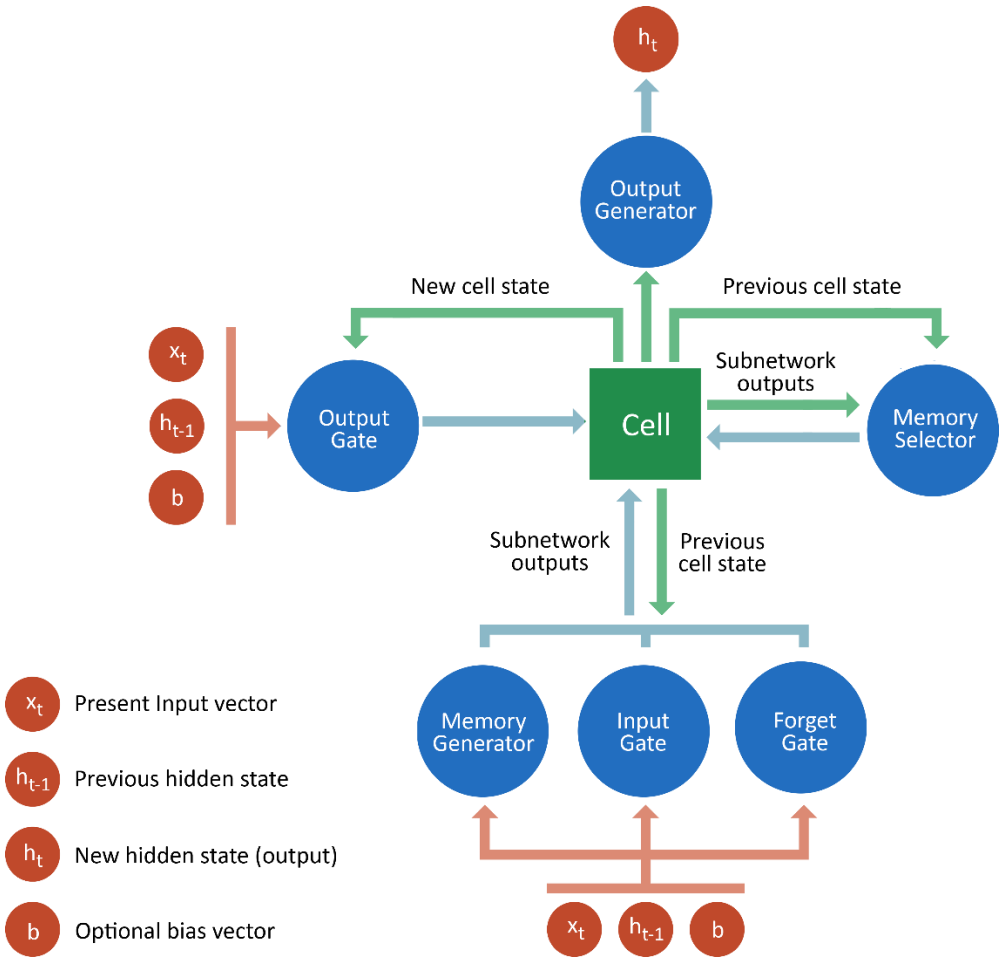

Figure S11. The architecture of a single long short-term memory (LSTM) cell block and the associated subnetworks. This figure outlines the workflow of an LSTM cell, which takes the previous memory cell state, the previous output state, and the input vector for the current time step as input. The forget gate decides which part of the old memory to forget and pushes it to the forgetting vector. The input gate decides the influence of the new input and the new memory generator generates a new memory vector for the current timestep; together, these two subnetworks are termed as the new memory valve. The operations of the forget gate and the new memory valve together update the memory cell state in the memory selector, which is then forwarded to the next time step. Finally, the output gate generates the current output vector, which is then updated in accordance with the new memory state to generate the new output hidden state, which becomes the output of the current time step.

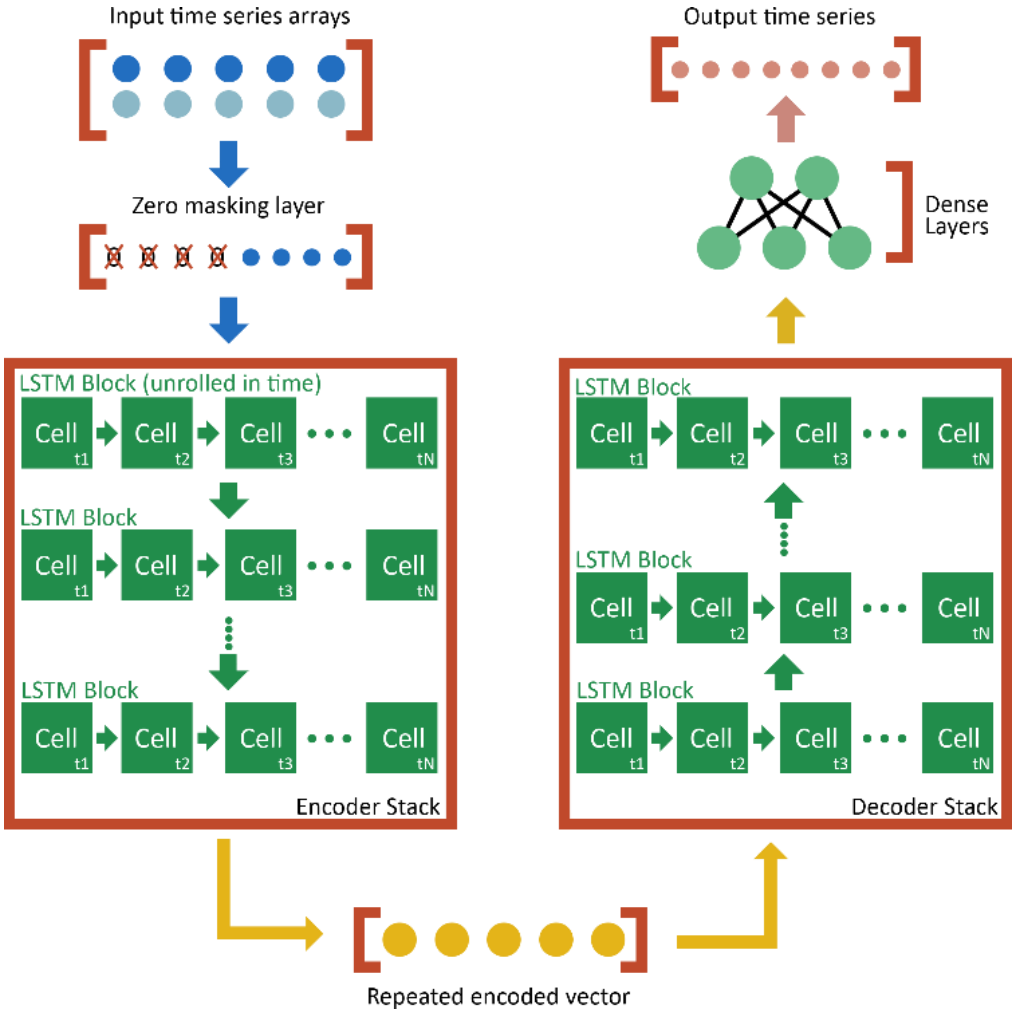

Figure S12. The layer-architecture of the sequence-to-sequence (S2S) model used in the paper. The input is first pushed to a zero masking layer which trims the leading zero paddings that are added to make the dataset uniform so that it is viable for batch training in TensorFlow, thus ensuring the model learns from only the actual data. The encoder and decoder blocks both contain four LSTM cell blocks, with each block containing 100 hidden nodes. The encoder takes the input from the masking layer and passes an encoded vector which is repeated and fed in each time step to the decoder, to generate the output sequence. Subsequently, the output sequence is passed to two densely connected layers, which optimize the predictions and outputs the final output sequence. The input size of the encoder is determined by the maximum size of the input sequences that are used to train the model, and the input size of the decoder is determined by the maximum size of the output sequences that are used as labels to train the model.

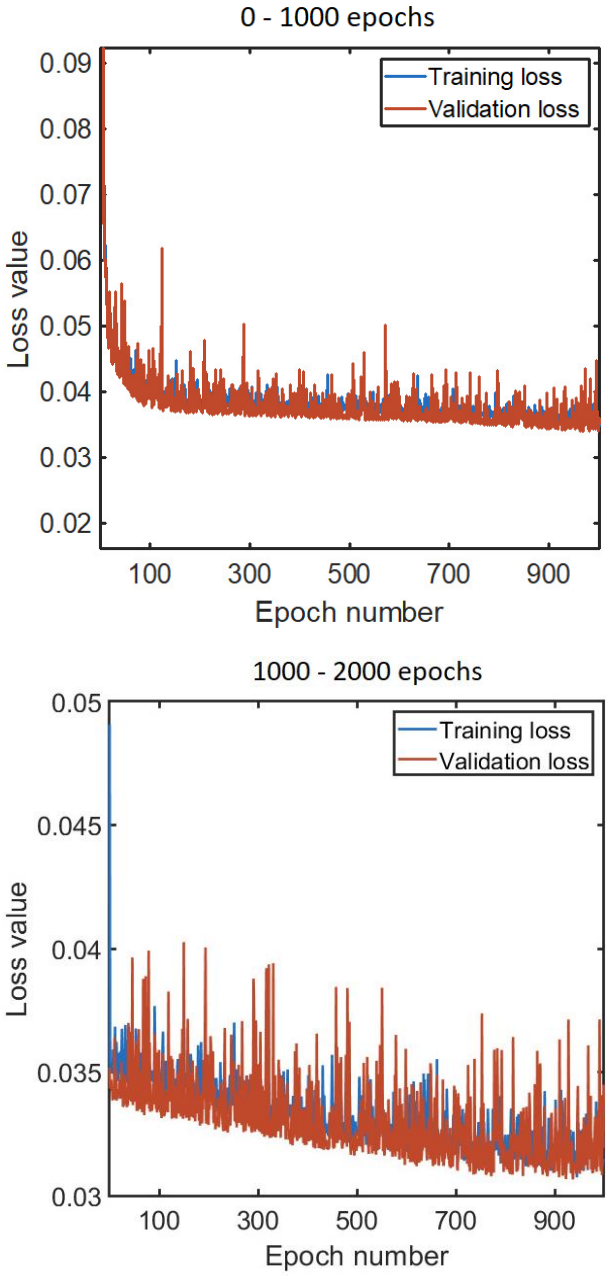

Figure S13. The two training phases of the model. The first phase has a larger learning rate of 0.0004 to converge to the approximate parameter region within 1000 epochs after which the model had seemingly settled with a training validation loss of around 0.04. The second phase training proved to be effective in lowering the training validation loss further by having a slower learning rate of 0.00025 to explore the possibility of minimizing the training validation loss within the region when trained for another period of 1000 epochs while checking for overfitting. Additionally, a random 15% of the training data was used as validation data for each epoch. The best validation loss achieved by the S2S network while training was 0.0312, after which further improvements were not seen. The training data contained 10497 samples from 42 cells, with a mini-batch processing size of 300 samples.

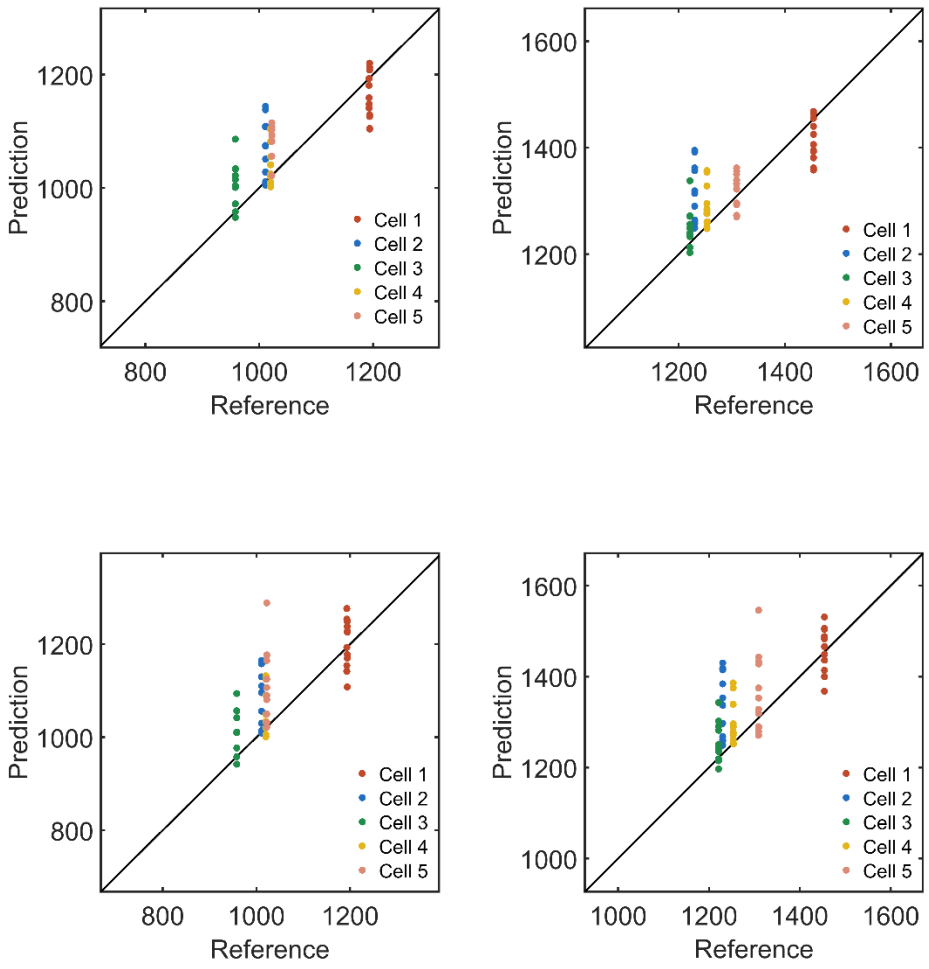

Figure S14. The prediction vs reference regression plots for the EOL80 and the EOL65 errors respectively, of all the five cells over various points in their lifetime. The top two figures show the EOL80 and EOL65 error metric for the normal validation scenario, while the bottom two figures show the same for the validation with noise scenario. The error variation in y-axis also serves to highlight the range of error over the lifetime of the cell.

Table S1. The error values of the four metrics in validation, namely the mean prediction error, the EOL80 error, the EOL65 error and the knee-point error, for both the normal validation and the noisy validation scenarios. The best-case and the worst-case cells are shown here, with the initial (100 cycle input), mean, median and the maximum error values.

Metric	Condition	Best-case	Worst-case
Validation with Normal Input			
MAPE [%]	Earliest	1.78	4.15
	Mean	1.19	3.12
	Median	1.13	3.10
	Max	2.47	6.23
EOL80 Error [cycles]	Earliest	81	128
	Mean	27	53
	Median	19	62
	Max	86	135
EOL65 error [cycles]	Earliest	27	78
	Mean	47	132
	Median	19	70
	Max	55	168
Knee-point error [cycles]	Earliest	85	274
	Mean	30	177
	Median	22	179
	Max	107	274
Validation with Noisy Input			
MAPE [%]	Earliest	0.67	4.88
	Mean	1.52	4.09
	Median	1.32	3.63
	Max	5.46	12.11
EOL80 Error [cycle]	Earliest	24	136
	Mean	37	70
	Median	17	61
	Max	133	267
EOL65 error [cycle]	Earliest	18	154
	Mean	37	98
	Median	24	86
	Max	134	285
Knee-point error [cycle]	Earliest	30	276
	Mean	51	205
	Median	33	199
	Max	165	314
Computation Time [s]	Mean	10	10

Table S2. The comparison between the iterative LSTM and the S2S model, in the mean MAPE and the other three metrics, namely the EOL80 error, EOL65 error and the knee-point error.

Metric	Condition	Best-case		Worst-case	
		S2S	**LSTM**	**S2S**	**LSTM**
MAPE [%]	Earliest	1.78	1.82	4.15	5.79
	Mean	1.19	1.78	3.12	4.49
	Max	2.47	2.98	6.23	6.69
EOL80 Error [cycle]	Earliest	81	87	128	156
	Mean	37	37	53	65
	Max	86	97	135	156
EOL65 error [cycle]	Earliest	47	83	132	164
	Mean	27	51	78	104
	Max	55	90	168	175
Knee-point error [cycle]	Earliest	85	122	274	290
	Mean	30	79	176	200
	Max	107	139	274	290
Computation time [s]	Max	10	150	10	150

Table S3. The specifications of the cells used in the ageing experiments.

Specification	Value
Cell	UR18650E
Type	Cylindrical
Chemistry (Anode / Cathode)	Graphite / NMC
Nominal capacity (of the batch used in the experiment)	1850 mAh
Weight	45.5 g
Manufacturer suggested charging protocol	CC-CV 1440 mA, 4.20 V, 3.0 hrs
Temperature (manufacturer's rating)	Charge: 0 to 45°C Discharge: -20 to +60°C Storage: -20 to +50°C
Volumetric energy density	432 Wh/L
Gravimetric energy Density	162 Wh/kg
Max. height	65.1 mm
Max. diameter	18.5 mm

Note S1: Calculation of the knee-point

The knee-points of the cells were calculated using a gradient change observation method. The original capacity curves of the 48 cells in the dataset were taken and the gradients of the curves were obtained from them using MATLAB's grad() function. Then, the value of the gradient, after which the change in the gradient accelerated, was observed. After getting the predicted capacity degradation curves, they were similarly processed to get their gradients and the previous value range obtained from the original curves was used to obtain the cycle numbers at which the gradients of the predicted curves also crossed the same value. This would be the indication of the knee-point in the predicted curve. The figure below shows a representative example of the process.

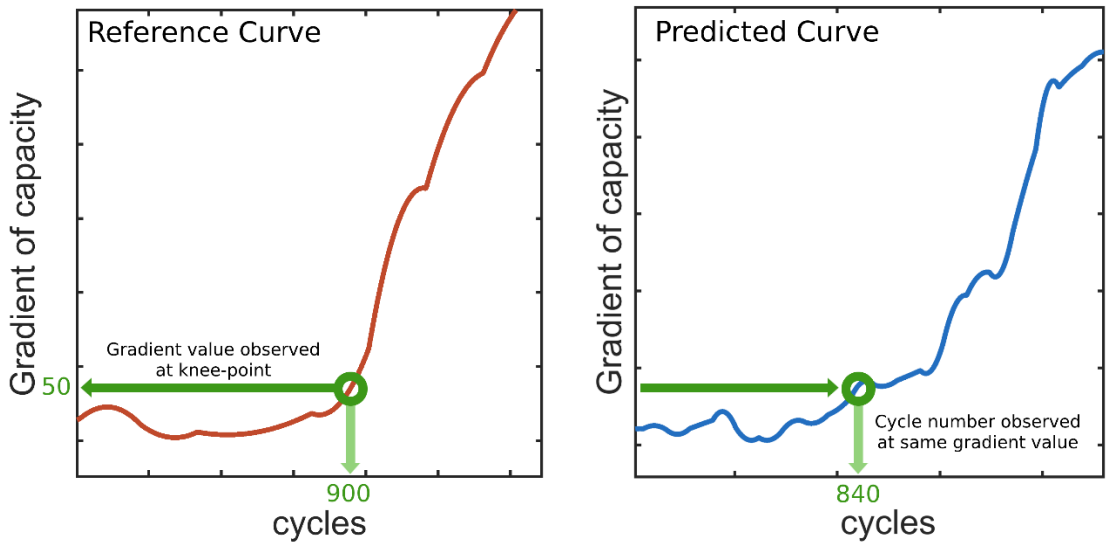

Figure S15. The process of calculating the knee-point for evaluation. The first gradient of capacity vs cycle curve is obtained from the original reference data, and the second curve is obtained from the predicted degradation curve from the model.